

The Kinetic Boundary Layer around an Absorbing Sphere and the Growth of Small Droplets

M. E. Widder¹ and U. M. Titulaer¹

Received December 1, 1988

Deviations from the classical Smoluchowski expression for the growth rate of a droplet in a supersaturated vapor can be expected when the droplet radius is not large compared to the mean free path of a vapor molecule. The growth rate then depends significantly on the structure of the kinetic boundary layer around a sphere. We consider this kinetic boundary layer for a dilute system of Brownian particles. For this system a large class of boundary layer problems for a planar wall have been solved. We show how the spherical boundary layer can be treated by a perturbation expansion in the reciprocal droplet radius. In each order one has to solve a finite number of *planar* boundary layer problems. The first two corrections to the planar problem are calculated explicitly. For radii down to about two velocity persistence lengths (the analog of the mean free path for a Brownian particle) the successive approximations for the growth rate agree to within a few percent. A reasonable estimate of the growth rate for all radii can be obtained by extrapolating toward the exactly known value at zero radius. Kinetic boundary layer effects increase the time needed for growth from 0 to 10 (or $2\frac{1}{2}$) velocity persistence lengths by roughly 35% (or 175%).

KEY WORDS: Droplet growth; kinetic boundary layer; Brownian motion; Klein-Kramers equation.

1. INTRODUCTION AND SURVEY

Consider a small liquid drop suspended in a gas mixture consisting of a supersaturated vapor and a background gas insoluble in the liquid. The droplet will grow by absorbing vapor molecules that diffuse toward it through the background gas. A simple theoretical treatment for problems of this type was proposed long ago by Smoluchowski⁽¹⁾: he solved the stationary diffusion equation for the concentration of vapor molecules with

¹ Institut für theoretische Physik, Johannes Kepler Universität Linz, A-4040 Linz, Austria.

the boundary condition of vanishing concentration at the surface of the droplet. This simplest treatment yields a growth rate inversely proportional to the droplet radius (a derivation will be given in Section 6). For small radii this result becomes nonsensical, and a more refined theoretical treatment is called for. For droplets of molecular dimensions a fully microscopic treatment is required; such a treatment is beyond the scope of the present paper. However, for droplets large compared to the critical droplet radius, but of a size comparable to the mean free path of the vapor molecules in the gas, a treatment based on a kinetic description of the gas, combined with simple boundary conditions at the droplet surface, appears promising. In this paper we explore the simplest model of this type. Some possible extensions are briefly discussed in Section 7; a further discussion of the underlying physics can be found, e.g., in a review by Wagner.⁽²⁾

The simplest kinetic equation is the Klein–Kramers equation⁽³⁾ for noninteracting Brownian particles; the simplest relevant boundary condition is obtained by assuming that any Brownian particle hitting the surface of the droplet is absorbed by it. This implies that just outside the surface there are no Brownian particles with radial velocities pointing outward from the surface. Thus, the velocity distribution near the surface must be far from Maxwellian: the droplet is surrounded by a *kinetic boundary layer*.⁽⁴⁾ The corresponding kinetic boundary layer problem for a flat boundary was solved exactly by Marshall and Watson.⁽⁵⁾ An equivalent treatment was given by Hagan *et al.*⁽⁶⁾ We presented an efficient numerical solution in a recent paper,⁽⁷⁾ henceforth referred to as I; this paper also contains more complete references to earlier work on the subject. For the spherical problem the situation is less satisfactory. There are a number of approximate treatments, based on truncations of a set of moment equations equivalent to the Klein–Kramers equation. The earliest treatment of this type was given by Razi Naqvi *et al.*,⁽⁸⁾ the most complete one by Kumar and Menon.⁽⁹⁾ Although in particular the latter paper provides quite accurate numerical values for not too small radii, the procedure remains somewhat unsatisfactory, since the truncation process involved requires a number of to some extent arbitrary choices.

The central result of the present paper is that the spherical boundary layer problem can be treated by means of a perturbation theory in the reciprocal droplet radius (in suitable dimensionless units). In lowest order we are led back to the known planar solution, and all subsequent correction terms can also be obtained from the solution of auxiliary *planar* boundary layer problems. Thus, each term in the perturbation series could in principle be determined analytically; in practice the numerical procedure from I can provide accurate results with much less effort.

The perturbation algorithm is described in Section 4. In preparation

we present the basic equations in Section 2; in particular, we transform the three-dimensional Klein–Kramers equation to a symmetry-adapted system of coordinates in the one-particle phase space. In Section 3 we construct the building blocks for the solution of the boundary layer problem, the boundary layer eigenfunctions. These are obtained as formal series in the inverse droplet radius R . In Section 4 we show how these functions should be linearly combined to provide the solution of the fundamental boundary layer problem. The first two correction terms are then explicitly evaluated in Section 5, the first one analytically, the second one numerically. To obtain a rough estimate of the quality of the approximation thus obtained, we compare with the exactly known limit $R \downarrow 0$. We also compare with some earlier numerical results, and with an approximate analytic expression by Sahni.⁽¹⁰⁾

In Section 6 we derive the consequences for the growth curves of droplets in a supersaturated vapor. In this context we propose a simple way to include the effect of finite supersaturation. In the final section we discuss some physical and mathematical limitations of our simple model and of our treatment of it, as well as some ways in which some of the neglected physical effects could be taken into account without an undue increase in mathematical complexity.

2. THE KLEIN–KRAMERS EQUATION IN SPHERICAL GEOMETRY

The kinetic equation for the joint distribution $P(\mathbf{u}, \mathbf{r}, t)$ of the velocity \mathbf{u} and the position \mathbf{r} of a Brownian particle (the Klein–Kramers equation) reads

$$\frac{\partial P(\mathbf{u}, \mathbf{r}, t)}{\partial t} = \left[-\mathbf{u} \cdot \frac{\partial}{\partial \mathbf{r}} + \gamma \frac{\partial}{\partial \mathbf{u}} \cdot \left(\mathbf{u} + \frac{1}{m\beta} \frac{\partial}{\partial \mathbf{u}} \right) \right] P(\mathbf{u}, \mathbf{r}, t) \quad (2.1)$$

where m is the mass of the particle, γ is its friction coefficient (i.e., the rate at which its velocity reaches equilibrium), and $\beta = (kT)^{-1}$, with T the temperature of the surrounding medium. In most of this paper we shall use dimensionless units with $\gamma = m\beta = 1$; this means in particular that the unit of length is the velocity persistence length $l = \gamma^{-1}(m\beta)^{-1/2}$. Moreover, we are interested in stationary solutions with spherical symmetry. Thus, it is convenient to use spherical coordinates for \mathbf{r} ,

$$(x_r, x_\theta, x_\phi) \equiv (r, \theta, \phi) \quad (2.2)$$

and to decompose \mathbf{u} according to the associated unit vectors:

$$u_r = \mathbf{u} \cdot \hat{e}_r(\mathbf{r}); \quad u_\theta = \mathbf{u} \cdot \hat{e}_\theta(\mathbf{r}); \quad u_\phi = \mathbf{u} \cdot \hat{e}_\phi(\mathbf{r}) \quad (2.3)$$

When one transforms (2.1) into an equation for $P(u_r, u_\theta, u_\phi; r, \theta, \phi; t)$, the implicit \mathbf{r} dependence of the u_k leads to the appearance of ‘‘covariant’’ derivatives:

$$\mathbf{u} \cdot \frac{\partial}{\partial \mathbf{r}} \Rightarrow \sum_k \frac{u_k}{|\partial \mathbf{r} / \partial x_k|} \frac{\partial}{\partial x_k} + \sum_{klm} \Gamma_{kl}^m u_k u_l \frac{\partial}{\partial u_m} \tag{2.4}$$

where the Γ_{kl}^m are the connection coefficients for the ‘‘noncoordinate basis’’ used, defined by Misner *et al.*⁽¹¹⁾ For the spherical coordinate system the only nonvanishing connection coefficients are (see ref. 11, p. 213)

$$\begin{aligned} \Gamma_{r\theta}^\theta &= \Gamma_{r\phi}^\phi = -\Gamma_{\theta\theta}^r = -\Gamma_{\phi\phi}^r = \frac{1}{r} \\ \Gamma_{\theta\phi}^\phi &= -\Gamma_{\phi\theta}^\theta = \frac{1}{r} \text{ctg } \theta \end{aligned} \tag{2.5}$$

Hence one obtains for the stationary version of (2.1)²

$$\begin{aligned} &\left[\frac{\partial}{\partial u_r} \left(\frac{\partial}{\partial u_r} + u_r \right) + \frac{\partial}{\partial u_\theta} \left(\frac{\partial}{\partial u_\theta} + u_\theta \right) + \frac{\partial}{\partial u_\phi} \left(\frac{\partial}{\partial u_\phi} + u_\phi \right) - u_r \frac{\partial}{\partial r} - \frac{u_\theta}{r} \frac{\partial}{\partial \theta} \right. \\ &\quad - \frac{u_\phi}{r \sin \theta} \frac{\partial}{\partial \phi} - \frac{1}{r} (u_\theta^2 + u_\phi^2) \frac{\partial}{\partial u_r} + \frac{1}{r} (u_r u_\theta - u_\phi^2 \text{ctg } \theta) \frac{\partial}{\partial u_\theta} \\ &\quad \left. + \frac{1}{r} (u_r u_\phi + u_\theta u_\phi \text{ctg } \theta) \frac{\partial}{\partial u_\phi} \right] P(u_r, u_\theta, u_\phi; r, \theta, \phi) = 0 \end{aligned} \tag{2.6}$$

In this paper we are concerned only with solutions of (2.6) that are spherically symmetric; hence, they do not depend on θ and ϕ , and they contain u_θ and u_ϕ only through the combination

$$u_t = (u_\theta^2 + u_\phi^2)^{1/2} \tag{2.7}$$

For such solutions (2.6) can be simplified to

$$\left[\mathcal{C}_r + \mathcal{C}_t - u_r \frac{\partial}{\partial r} - \frac{1}{r} \left(u_t^2 \frac{\partial}{\partial u_r} - u_r u_t \frac{\partial}{\partial u_t} \right) \right] P(u_r, u_t, r) = 0 \tag{2.8}$$

with

$$\mathcal{C}_r = \frac{\partial}{\partial u_r} \left(u_r + \frac{\partial}{\partial u_r} \right); \quad \mathcal{C}_t = \frac{1}{u_t} \frac{\partial}{\partial u_t} u_t \left(u_t + \frac{\partial}{\partial u_t} \right) \tag{2.9}$$

²The ‘‘covariant’’ additional terms were omitted in an earlier treatment by Kneller and Titulaer,⁽¹²⁾ the moment equations derived there are correct, however, due to a cancellation of errors.

The operators \mathcal{C}_r and \mathcal{C}_l already occurred in I; their eigenvalues and eigenfunctions are given by

$$\mathcal{C}_r \phi_m(u_r) = -m \phi_m(u_r); \quad \mathcal{C}_l \chi_l(u_l) = -2l \chi_l(u_l) \quad (2.10)$$

where m and l may assume all nonnegative integer values and ϕ_m and χ_l are known functions, given explicitly in I. For later reference we merely note that $\phi_0(u_r)$ and $\chi_0(u_l)$ correspond to the Maxwell distribution, and that $\phi_1(u_r)$ is the only one of the $\phi_m(u_r)$ that carries a radial current (of unit density in the positive r direction). The operator \mathcal{C}_r can be written in the form^(13,7)

$$\mathcal{C}_r = -a_+ a_-; \quad a_+ \phi_m = (m+1) \phi_{m+1}; \quad a_- \phi_m = (1 - \delta_{m0}) \phi_{m-1} \quad (2.11)$$

It will turn out to be convenient to introduce similar raising and lowering operators for the χ_l :

$$b_+ \chi_l = 2(l+1) \chi_{l+1}; \quad b_- \chi_l = 2l \chi_{l-1} \quad (2.12)$$

The explicit form of the b_{\pm} can be deduced from the explicit expressions in I and the properties of the Laguerre polynomials. For present purposes we merely note the relations

$$u_l^2 \frac{\partial}{\partial u_r} = a_+ (b_+ + b_- + 2\mathcal{C}_l - 2) \quad (2.13a)$$

$$u_r u_l \frac{\partial}{\partial u_l} = (a_+ + a_-)(b_+ + \mathcal{C}_l - 2) \quad (2.13b)$$

that will be useful in constructing special solutions of (2.8).

3. THE BOUNDARY LAYER EIGENFUNCTIONS

In this section we introduce a set of special solutions of (2.8) that will be used in constructing solutions of boundary value problems in spherical geometry. First there is the obvious equilibrium solution

$$\Psi_0(u_r, u_l, r) = \phi_0(u_r) \chi_0(u_l) \quad (3.1)$$

which corresponds to a unit density for all \mathbf{r} . Second, there is a current-carrying solution Ψ_c , which can formally be written as⁽¹⁰⁾

$$\Psi_c(u_r, u_l, r) = \sum_{i=0}^{\infty} \frac{-i!}{r^{i+1}} \sum_{l=0}^{[i/2]} \frac{1}{2^l l!} \chi_l(u_l) \phi_{i-2l}(u_r) \quad (3.2)$$

where $[i/2]$ denotes the integer part of $i/2$. The first sum in (3.2) diverges for $|u_r| > r$, but (3.2) can be used to obtain moments of Ψ_c , e.g., the density $n_c(r) = -r^{-1}$ and the current $j_c(r) = -r^{-2}$. Since we shall need only finite approximants to the infinite sum in (3.2), we shall not need expressions for Ψ_c of more general validity, which can be obtained from (3.2) by analytic continuation.

From the results obtained in I for the planar boundary layer problem (and, e.g., from the relation between one-dimensional and spherical problems in quantum mechanics or electromagnetism) one expects additional solutions of (2.8) that for large r have the form

$$\tilde{\Psi}_{nl}(u_r, u_t, r) \simeq \frac{1}{r} e^{-\lambda_{nl}r} \psi_{nl}(u_r) \chi_l(u_t); \quad \lambda_{nl} = (n + 2l)^{1/2} \quad (3.3)$$

The explicit form of the $\psi_{nl}(u)$ is given in Section 4 of I. From (3.2) we suspect that the full boundary layer functions of the three-dimensional problem contain a mixture of different l ; all terms should, however, have the same inverse decay lengths λ_{nl} . Hence we use a somewhat different labeling system and search for solutions of the form

$$\Psi^{nL}(u_r, u_t, r) = e^{-r\sqrt{\nu}n} \sum_{i=i_0}^{\infty} \frac{1}{r^i} \Psi_i^{nL}(u_r, u_t) \quad (n = 1, 2, 3, \dots) \quad (3.4a)$$

with

$$\Psi_i^{nL}(u_r, u_t) = \sum_{l=0}^{\infty} \chi_l(u_t) \Phi_{il}^{nL}(u_r) \quad (3.4b)$$

(the meaning of the index L will become clear as the construction proceeds). Substituting (3.4a) into (2.8) and using the results (2.9)–(2.13) leads to the set of equations

$$\begin{aligned} & [\mathcal{C}_r + \mathcal{C}_t + n^{1/2}(a_+ + a_-)] \Psi_i^{nL} \\ &= [-b_+ a_- + (\mathcal{C}_t + 1 - i) a_+ - (\mathcal{C}_t + i - 3) a_- + b_- a_+] \Psi_{i-1}^{nL} \end{aligned} \quad (3.5)$$

This hierarchy of equations can be solved consecutively when the operator acting on Ψ_i^{nL} on the left-hand side can be inverted. The expansion (3.4b) effectively reduces \mathcal{C}_t to a number. A similar reduction for the remaining part of the operator can be obtained by expanding the $\Phi_{il}^{nL}(u_r)$ in terms of the eigenfunctions of

$$\mathcal{C}_{rn} = \mathcal{C}_r + n^{1/2}(a_+ + a_-) = -[(a_+ - n^{1/2})(a_- - n^{1/2}) - n] \quad (3.6)$$

Since the a_{\pm} obey the familiar harmonic oscillator commutation relations, the eigenvalues of \mathcal{C}_{rn} are

$$\mu_{nm} = n - m \quad (m = 0, 1, 2, \dots) \tag{3.7}$$

The eigenfunctions are related to those of a harmonic oscillator shifted over $(2n)^{1/2}$; using the method of Pagani,^(14,15) one finds³

$$\zeta_{nm}(u_r) = \text{cst} \cdot H_m \left\{ \frac{1}{\sqrt{2}} [u_r - (2n)^{1/2}] \right\} e^{-(u_r - \sqrt{2n})^2/2} \tag{3.8}$$

A comparison with the definition in I of the $\psi_{nl}(u_r)$ occurring in (3.3) yields the relation

$$\psi_{nl}(u_r) = \text{cst} \cdot \zeta_{n+2l,n}(u_r) \tag{3.9}$$

The constant can be made equal to unity by a normalization convention for the ζ_{nm} . The normalization for the ψ_{nl} is⁽⁷⁾

$$\int \psi_{nl}(u_r) du_r = 1 \tag{3.10}$$

To obtain the same normalization for the ζ_{nm} , we introduce the raising and lowering operators

$$A_{n+} = 1 - a_+/\sqrt{n}; \quad A_{n-} = 1 - a_-/\sqrt{n} \tag{3.11}$$

and require

$$A_{n+} \zeta_{nm} = \zeta_{n,m+1}; \quad \zeta_{m0} = \psi_{n0} \tag{3.12}$$

Since a_+ is a multiple of $\partial/\partial u_r$,⁽⁷⁾ this ensures that A_{n+} preserves the normalization condition (3.10). For the action of A_{n-} one finds

$$A_{n-} \zeta_{nm} = (m/n) \zeta_{n,m-1} \tag{3.13}$$

We now return to (3.4) and insert in (3.4b) the additional decomposition

$$\Phi_{il}^{nL}(u_r) = \sum_{m=0}^{\infty} f_{ilm}^{nL} \zeta_{nm}(u_r) \tag{3.14}$$

³ The specific form of the exponential results from the factor $\exp(-u_r^2/2)$ multiplying the harmonic oscillator eigenfunctions.⁽¹³⁾

From (3.5) one then obtains a set of equations for the f_{ilm}^{nL} :

$$\begin{aligned}
 (n - m - 2l) f_{ilm}^{nL} &= 2(l + 1) n^{1/2} [f_{i-1, l+1, m}^{nL} - f_{i-1, l+1, m-1}^{nL}] \\
 &\quad - 2l(n)^{1/2} \left[f_{i-1, l-1, m}^{nL} - \frac{m+1}{n} f_{i-1, l-1, m+1}^{nL} \right] \\
 &\quad + n^{1/2} \left[(-1 + i + 2l) f_{i-1, l, m-1}^{nL} + (4 - 2i) f_{i-1, l, m}^{nL} \right. \\
 &\quad \left. + (-3 + i - 2l) \frac{m+1}{n} f_{i-1, l, m+1}^{nL} \right] \tag{3.15}
 \end{aligned}$$

where we used the convention

$$f_{ilm}^{nL} = 0 \quad \text{for } l < 0 \text{ or } m < 0 \tag{3.16}$$

The set of equations (3.15) is solvable provided the right-hand side vanishes for $m = n - 2l$; on the other hand, it leaves the $f_{il, n-2l}^{nL}$ undetermined. This ambiguity can be resolved by requiring that the solvability condition shall be satisfied *in order* $i + 1$. Thus, $f_{il, n-2l}^{nL}$ is determined by putting $m = n - 2l$ in the rhs of (3.15), replacing $i - 1$ by i throughout, and putting the result equal to zero. This allows one to determine the $f_{il, n-2l}^{nL}$ (none of the other $f_{i'l'm'}^{nL}$ occurring in this relation obeys the resonance condition $m' + 2l' = n$). A simple example of the calculation sketched above will be given in Section 5.

Next we consider the start of the recursion scheme. At order i_0 the right-hand side of (3.15) vanishes by definition. There are $[n/2] + 1$ independent solutions, which we choose to be

$$f_{i_0 l m}^{nL} = \delta_{lL} \delta_{m, n-2L} \quad (0 \leq L \leq [n/2]) \tag{3.17}$$

i.e., all $f_{i_0 l m}^{nL}$ obey the resonance condition. (Moreover, no solutions are obtained for noninteger n .) At order $i_0 + 1$, and for a resonant index pair (l, m) , the right-hand side of (3.15) reduces to $(4 - 2i_0 - 2) f_{i_0 l m}^{nL}$, and the solubility condition is violated unless we choose

$$i_0 = 1 \tag{3.18}$$

[since different (l, m) do not couple, nothing is gained by considering linear combinations of the solutions (3.17)]. Thus, the only possible solutions of type (3.4) have the asymptotic behavior (3.3), as we conjectured.

Further inspection shows that nonvanishing f_{ilm}^{nL} occur only for

$$\begin{aligned}
 \max[0, L - i + 1] &\leq l \leq L + i - 1 \\
 \max[0, n - 2L - i + 1] &\leq m \leq n - 2L + i - 1
 \end{aligned} \tag{3.19}$$

Thus, only a finite number of new coefficients appear in each order; this will be crucial for the solution of the boundary value problem.

To conclude this section, we mention two important properties of the solutions Ψ^{nL} . First, the associated current density

$$\mathbf{j}^{nL}(r) \equiv \int d\mathbf{u} \mathbf{u} \Psi^{nL}(u_r, u_t, r) \tag{3.20}$$

as for any solution of (2.1), must have vanishing divergence, hence be a constant or a multiple of r^{-2} . Both possibilities are excluded by the ansatz (3.4); hence $\mathbf{j}^{nL}(r)$ vanishes, and in particular

$$j_r^{nL}(r) = \int d\mathbf{u} u_r \Psi^{nL}(u_r, u_t, r) = 0 \tag{3.21}$$

Second, our calculations showed, in all cases considered, that the density associated with Ψ^{nL} is determined completely by the contributions of order $i = 1$; hence

$$n^{nL}(r) \equiv \int d\mathbf{u} \Psi^{nL}(u_r, u_t, r) = \frac{1}{r} e^{-r\sqrt{\gamma}n} \delta_{L0} \tag{3.22}$$

We did not succeed in finding a general proof; our later use of the relation, however, involves only orders in i for which the relation was checked explicitly.

4. THE REDUCTION OF THE SPHERICAL BOUNDARY LAYER PROBLEM

The problem addressed in this section is the construction of the Milne solution P_M of (2.8), satisfying the boundary conditions

$$\lim_{r \rightarrow \infty} P_M(u_r, u_t, r) = \text{cst} \cdot \Psi_0(u_r, u_t) \tag{4.1a}$$

$$P_M(u_r, u_t, R) = 0 \quad \text{for } u_r > 0 \tag{4.1b}$$

The normalization of the solution might be fixed by specifying the constant in (4.1a), but mathematically it is slightly more convenient to fix the total incoming current density:

$$\int d\mathbf{u} u_r P_M(u_r, u_t, R) = -1 \tag{4.1c}$$

Our solution strategy will be to reduce the spherical problem to a sequence of planar boundary layer problems. It is therefore convenient to use instead

of the Ψ_0 , Ψ_c , and Ψ^{nL} of Section 3 the slightly modified set of basic solutions

$$\Phi_0(u_r, u_t, r) = \Psi_0(u_r, u_t, r) \tag{4.2a}$$

$$\Phi_c(u_r, u_t, r) = R^2\Psi_c(u_r, u_t, r) + R\Psi_0(u_r, u_t, r) \tag{4.2b}$$

$$\Phi^{nL}(u_r, u_t, r) = e^{R\sqrt[n]{n}}R\Psi^{nL}(u_r, u_t, r) \tag{4.2c}$$

For $R \gg 1$ these functions, considered as functions of $r - R$, correspond to the $\Psi_0(u_x, u_t, x)$, $\Psi_c(u_x, u_t, x)$, and $\Psi_{n-2L,L}(u_x, x) \chi_L(u_t)$ of I, respectively.

We now try to satisfy the conditions (4.1) by a linear combination of the functions (4.2). From (4.1c) one sees that the coefficient of Φ_c must be unity. The other coefficients are written as power series in R^{-1} ; the resulting ansatz is

$$P_M = \left(\alpha_0^0 + \frac{1}{R} \alpha_1^0 + \frac{1}{R^2} \alpha_2^0 + \dots \right) \Phi_0 + \Phi_c + \sum_{nL} \left(\alpha_0^{nL} + \frac{1}{R} \alpha_1^{nL} + \frac{1}{R^2} \alpha_2^{nL} + \dots \right) \Phi^{nL} \tag{4.3}$$

The coefficients α_i^0 and α_i^{nL} will be determined consecutively by satisfying (4.1b) order by order in R^{-1} , using the expansions (3.2) and (3.4) for Ψ_c and the Ψ^{nL} . Moreover, since (4.1b) must hold for all u_t , and the $\chi_i(u_t)$ are a complete set of functions of u_t , the condition (4.1b) must hold for the coefficients of each one of the χ_i separately. In order R^0 one so obtains the set of equations

$$\alpha_0^0 \phi_0(u_r) - \phi_1(u_r) + \sum_n \alpha_0^{n0} \Phi_{10}^{n0}(u_r) = 0 \quad \text{for } u_r > 0 \tag{4.4a}$$

$$\sum_n \alpha_0^{nL} \Phi_{1L}^{nL}(u_r) = 0 \quad \text{for } u_r > 0; \quad L \geq 1 \tag{4.4b}$$

with $\Phi_{iL}^{nL}(u_r)$ defined in (3.4b), and further specified in (3.14). From (3.15) and (3.12a) we conclude

$$\Phi_{10}^{n0}(u_r) = \zeta_{m0}(u_r) = \psi_{n0}(u_r) \tag{4.5}$$

Hence (4.4a) reduces to the classical Milne problem, discussed in I, for which both exact and accurate numerical solutions are known. In particular we have

$$\alpha_0^0 \equiv x_M = -\zeta(1/2) = 1.46035\dots \tag{4.6a}$$

where $\zeta(x)$ denotes the Riemann ζ -function, and

$$\alpha_0^0 + \sum_n \alpha_0^{n0} \equiv n_M(0) \simeq 0.93611 \tag{4.6b}$$

(The latter quantity is equal to the density at the wall.) The α_0^{n0} are available in numerical form.^(7,16) The $\Phi_{1L}^{nL}(u_r)$ are identical with the $\zeta_{n,n-2L}(u_r)$ introduced in Section 3; they are complete on $u_r > 0$,^(17,5) hence (4.4b) implies

$$\alpha_0^{nL} = 0 \quad \text{for } L \geq 1 \tag{4.7}$$

The equations corresponding to (4.4) in order R^{-1} are

$$\alpha_1^0 \phi_0 - 2\phi_2 + \sum_n [\alpha_1^{n0} \Phi_{10}^{n0} + \alpha_0^{n0} \Phi_{20}^{n0}] = 0; \quad u_r > 0 \tag{4.8a}$$

$$-\phi_0 + \sum_n [\alpha_1^{n1} \Phi_{11}^{n1} + \alpha_0^{n0} \Phi_{21}^{n0}] = 0; \quad u_r > 0 \tag{4.8b}$$

$$\sum_n \alpha_1^{nL} \Phi_{1L}^{nL} = 0 \quad \text{for } L \geq 2; \quad u_r > 0 \tag{4.8c}$$

In the next order the corresponding expressions are

$$\alpha_2^0 \phi_0 - 6\phi_3 + \sum_n [\alpha_2^{n0} \Phi_{10}^{n0} + \alpha_1^{n0} \Phi_{20}^{n0} + \alpha_0^{n0} \Phi_{30}^{n0} + \alpha_1^{n1} \Phi_{20}^{n1}] = 0; \quad u_r > 0 \tag{4.9a}$$

$$-3\phi_1 + \sum_n [\alpha_2^{n1} \Phi_{11}^{n1} + \alpha_1^{n1} \Phi_{21}^{n1} + \alpha_0^{n0} \Phi_{21}^{n0} + \alpha_0^{n0} \Phi_{31}^{n0}] = 0; \quad u_r > 0 \tag{4.9b}$$

$$\sum_n [\alpha_2^{n2} \Phi_{12}^{n2} + \alpha_1^{n1} \Phi_{22}^{n1} + \alpha_0^{n0} \Phi_{32}^{n0}] = 0; \quad u_r > 0 \tag{4.9c}$$

$$\sum_n \alpha_2^{nL} \Phi_{1L}^{nL} = 0 \quad \text{for } L \geq 3; \quad u_r > 0 \tag{4.9d}$$

The general structure of the hierarchy becomes clear: from the last equation of each set one concludes

$$\alpha_i^{nL} = 0 \quad \text{for } L > i \tag{4.10}$$

The remaining equations have the structure

$$\alpha_i^0 \delta_{L0} \phi_0(u_r) + \sum_n \alpha_i^{nL} \Phi_{1L}^{nL}(u_r) = g_i^L(u_r) \quad \text{for } u_r > 0 \tag{4.11}$$

where $g_i^L(u_r)$ is a known function, expressible in the α_j^{nL} with $j < i$ and the Φ_{ji}^{nL} that were constructed in Section 3. In view of the relation

$$\Phi_{1L}^{nL}(u_r) = \zeta_{n,n-2L}(u_r) = \psi_{n-2L,L}(u_r) \tag{4.12}$$

this is the problem of finding the linear combination of the $\psi_{nL}(u_r)$ [and $\phi_0(u_r)$ for $L=0$] that matches $g_i^L(u_r)$ for $u_r > 0$. This in turn is the albedo problem treated in Section 4 of I, a problem for which a unique exact solution exists in principle, and an accurate numerical solution is available. Thus, each order in the hierarchy (4.8), (4.9), etc., can be reduced to a set of solvable planar boundary problems. In the next section we show that (4.8a) can again be reduced to the classical planar Milne problem; we also present some aspects of our numerical solution of (4.8b) and (4.9a).

5. EXPLICIT LOW-ORDER RESULTS

To solve (4.8a), we first construct Φ_{20}^{n0} , using the procedure outlined in Section 3. The starting point is (3.5) for $i=2$. Separating the l -components and using the fact that Ψ_1^{n0} has only an $l=0$ contribution, one obtains the equations

$$\mathcal{C}_{rn} \Phi_{20}^{n0} = (a_- - a_+) \Phi_{10}^{n0}; \quad [\mathcal{C}_{rn} - 2] \Phi_{21}^{n0} = -2a_- \Phi_{10}^{n0} \tag{5.1}$$

To obtain solutions, one expresses the right-hand sides in terms of the eigenfunctions ζ_{nm} of \mathcal{C}_{rn} , with eigenvalues $n - m$, using (3.11)–(3.13):

$$(a_- - a_+) \Phi_{10}^{n0} = n^{1/2}(-\zeta_{n,n-1} + \zeta_{n,n+1}) \tag{5.2a}$$

$$-2a_- \Phi_{10}^{n0} = 2(n)^{1/2}(\zeta_{n,n-1} - \zeta_{nn}) \tag{5.2b}$$

The relations (5.1) can now be inverted and give

$$\Phi_{20}^{n0} = -(n)^{1/2}(\zeta_{n,n-1} + \zeta_{n,n+1}) + f_{20n}^{n0} \zeta_{nn} \tag{5.3a}$$

$$\Phi_{21}^{n0} = n^{1/2}(-2\zeta_{n,n-1} + \zeta_{nn}) + f_{21,n-2}^{n0} \zeta_{n,n-2} \tag{5.3b}$$

The coefficients f_{20n}^{n0} and $f_{21,n-2}^{n0}$ can be determined by putting the right-hand side of (3.15) for f_{30n}^{n0} and $f_{31,n-2}^{n0}$ equal to zero. The other coefficients needed can be read off from (5.3); the results are

$$\Phi_{20}^{n0} = -(n)^{1/2}(\zeta_{n,n-1} - 2\zeta_{nn} + \zeta_{n,n+1}) = (a_+ + a_-) \Phi_{10}^{n0} \tag{5.4a}$$

$$\Phi_{21}^{n0} = n^{1/2}(\zeta_{nn} - 2\zeta_{n,n-1} + \zeta_{n,n-2}) = \frac{1}{\sqrt{n}} a_-^2 \Phi_{10}^{n0} \tag{5.4b}$$

The first relation can be used to simplify the last term in (4.8a) by exploiting (4.4a)⁴

$$\sum_n \alpha_0^{n0} \Phi_{20}^{n0} = \sum_n \alpha_0^{n0} (a_+ + a_-) \Phi_{10}^{n0} = (a_+ + a_-)(\phi_1 - \alpha_0^0 \phi_0) \quad \text{for } u_r > 0 \tag{5.5}$$

Using (2.10), we can now rewrite (4.8a) as

$$(\alpha_1^0 + 1) \phi_0 - \alpha_0^0 \phi_1 + \sum_n \alpha_1^{n0} \Phi_{10}^{n0} = 0 \quad \text{for } u_r > 0 \tag{5.6}$$

and a comparison with (4.4a) yields the solution

$$\alpha_1^0 = (\alpha_0^0)^2 - 1 = 1.13264\dots; \quad \alpha_1^{n0} = \alpha_0^0 \alpha_0^{n0} \tag{5.7}$$

For the first correction to the density at the wall one obtains

$$n_M^1 = \alpha_1^0 + \sum_n \alpha_1^{n0} = \alpha_0^0 n_M(0) - 1 \simeq 0.36705 \tag{5.8}$$

Some of the terms occurring in the other equations in (4.8) and (4.9) can be transformed in a similar way, but (as yet) not all. We therefore solved these equations numerically, using the procedure described in I. The main results are

$$\alpha_2^0 = -0.2660 \pm 0.0001 \tag{5.9a}$$

$$n_M^2 \equiv \alpha_2^0 + \sum_n \alpha_2^{n0} = -0.3346 \pm 0.0001 \tag{5.9b}$$

Two important aspects of the solution so obtained are the density at infinity, for which we obtain from (4.3) and (4.2b)

$$n_\infty^{[1]}(R) = R + \alpha_0^0 + \frac{1}{R} \alpha_1^0 + \frac{1}{R^2} \alpha_2^0 + \dots \tag{5.10}$$

and the density at the surface of the sphere, determined with the aid of the identity (3.22),

$$n_R^{[1]}(R) = n_M(0) + \frac{1}{R} n_M^1 + \frac{1}{R^2} n_M^2 + \dots \tag{5.11}$$

⁴ It is not trivial that, e.g., $(a_+ + a_-)$ may be interchanged with the summation, but we checked it, both analytically and numerically.

Both quantities are calculated for unit incoming current per unit area, which is indicated by the superscript [1]. The reciprocal of (5.10),

$$k(R) = [n_{\infty}^{[1]}(R)]^{-1} \tag{5.12}$$

is the current density at the surface per unit density at $r \rightarrow \infty$, i.e., the effective rate of the accretion reaction.

Thus far we have calculated only a few terms in the expansion in R^{-1} , and not much can be said about the convergence of the series. A first rough impression can be obtained from the plots of $k(R)$ and $n_R^{[1]}(R)$ as functions of R , shown in Figs. 1 and 2, respectively. For $R \geq 2$, consecutive approximations do not differ too much, and the result should be reliable. As an additional check, we consider the limit $R \downarrow 0$. Then the sphere becomes too small to affect the velocity distribution of the incoming particles to any significant extent, and we may assume

$$P_M(u_r, u_t, R) \simeq \phi_0(u_r) \chi_0(u_t) \Theta(-u_r) n_{\infty} \tag{5.13}$$

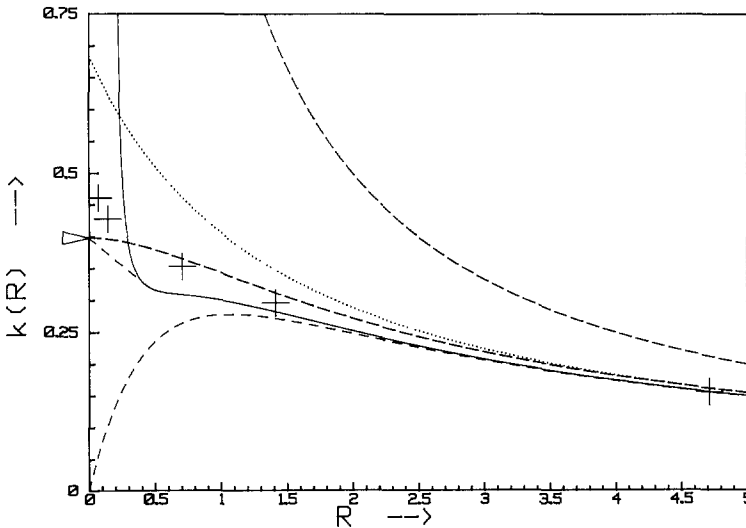


Fig. 1. Various approximations to the growth rate $k(R)$ of a droplet of radius R (in dimensionless units). The upper dashed, dotted, lower dashed, and solid curves are obtained by approximating $n_{\infty}^{[1]}$ in (5.12) by one, two, three, and four terms in (5.10), respectively. The long-dashed curve is Sahni's approximate analytic expression;⁽¹⁰⁾ the crosses denote moment calculations by Kumar and Menon.⁽⁹⁾ The arrow denotes the exact result for $R=0$; the tangent line to our best approximate result is used in constructing an approximate growth curve in Fig. 3.

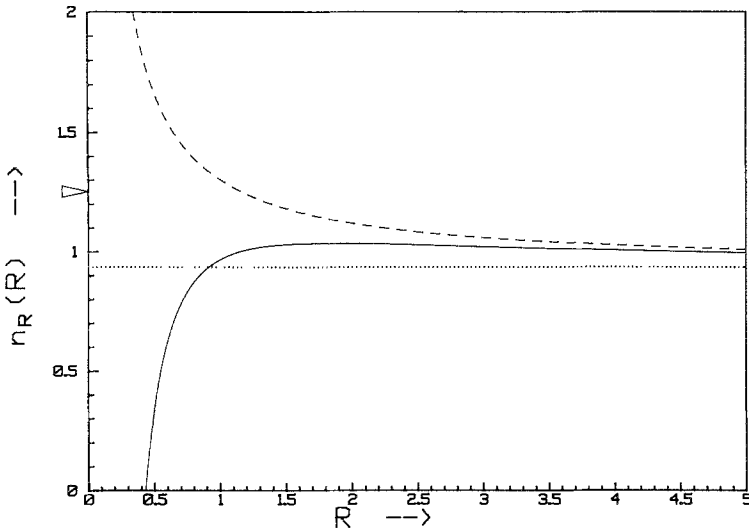


Fig. 2. The density at the surface of the sphere for unit incoming current density as a function of its radius, as calculated by taking one (dotted curve), two (dashed curve), and three (solid curve) terms in (5.11). The arrow denotes the exact result for $R=0$. We use dimensionless units, defined in Section 2.

The incoming current is easily calculated, and we obtain for the plotted quantities

$$\begin{aligned}
 k(R=0) &= (2\pi)^{-1/2} \simeq 0.39894\dots \\
 n_R^{[1]}(R=0) &= \frac{1}{2}(2\pi)^{1/2} = 1.25331\dots
 \end{aligned}
 \tag{5.14}$$

These results are indicated by arrows in the figures. Also included in Fig. 1 are the approximate analytic expression proposed by Sahni⁽¹⁰⁾ and numerical results by Kumar and Menon⁽⁹⁾ for some values of R . Both earlier results agree well with ours for not too small R values,⁵ but for $R \simeq 1$ our best approximants lie clearly lower.

6. THE GROWTH OF SMALL DROPLETS

The model treated in the preceding sections can be made into a model of droplet growth if we assume that each arriving Brownian particle increases the volume of the droplet by an amount v_0 . For a completely

⁵ Attempts to obtain better results by including more and more moments in a treatment similar to the one in ref. 9 were not successful. From a certain order, the approximants start to diverge, reflecting the divergence of the series (3.2). This behavior was predicted by Waldenström and Razi Naqvi.⁽¹⁹⁾

absorbing droplet in a medium with a density of Brownian particles approaching n_∞ for $r \rightarrow \infty$ we obtain

$$\frac{d}{dt} \left(\frac{4}{3} \pi R^3 \right) = 4\pi R^2 v_0 n_\infty k(R) \quad (6.1)$$

In standard units one has an extra factor $(m\beta\gamma)^{-1}$; in view of the Einstein relation this is precisely the diffusion coefficient D . The droplet radius thus obeys the equation⁶

$$\frac{dR}{dt} = Dv_0 n_\infty k(R) = \frac{Dv_0 n_\infty}{R + \alpha_0^0 l + \alpha_1^0 R^{-1} l^2 + \alpha_2^0 R^{-2} l^3 + \dots} \quad (6.2)$$

where l is the velocity persistence length defined after (2.1). Thus, the quantity plotted in Fig. 1 is proportional to the R -dependent growth rate of the droplet. The Smoluchowski approximation is obtained by replacing the denominator in (6.2) by R ; it yields the familiar growth law

$$R_S(t) = [2Dv_0 n_\infty (t - t_0)]^{1/2} \quad (6.3)$$

which leads to a, physically unacceptable, infinite growth rate at $R = 0$. In Fig. 3 we compare the curve (6.3) with those obtained by taking successively more terms in the denominator of (6.2) into account; we also show the result of the extrapolation to the known rate for $R = 0$ via the tangent construction shown in Fig. 1. Including the first correction term increases the time needed for growth from $R = 0$ to $R = 10l$ by 30%. Including two more terms plus the extrapolation to $R = 0$ adds a further 6%. The even more drastic effects on the growth time up to $R = 2.5l$ are shown in the figure.

Thus far we assumed that the droplet does not release any of the Brownian particles back into the medium. If the Brownian particles are to represent vapor molecules, this is not very realistic, except at extremely high supersaturation. If we maintain the assumption that each vapor particle hitting the droplet sticks to it at least long enough to become completely thermalized, and assume that the emission is thermal and does not depend on the concentration of vapor molecules in the gas (which must be

⁶ In deriving (6.2), we have assumed that the current can at any stage be determined from a *stationary* solution of the Klein-Kramers equation (2.1). This is justified as long as the growth rate in (6.2) stays much smaller than the thermal velocity of the Brownian particles. To check this, we note that the denominator of (6.2) is always larger than l . Thus, the ratio of (6.2) to the thermal velocity stays smaller than $v_0 n_\infty$, the volume fraction of the gas (at $r = \infty$) occupied by the Brownian particles. This quantity must be very small for a description in terms of *noninteracting* Brownian particles to make any sense at all.

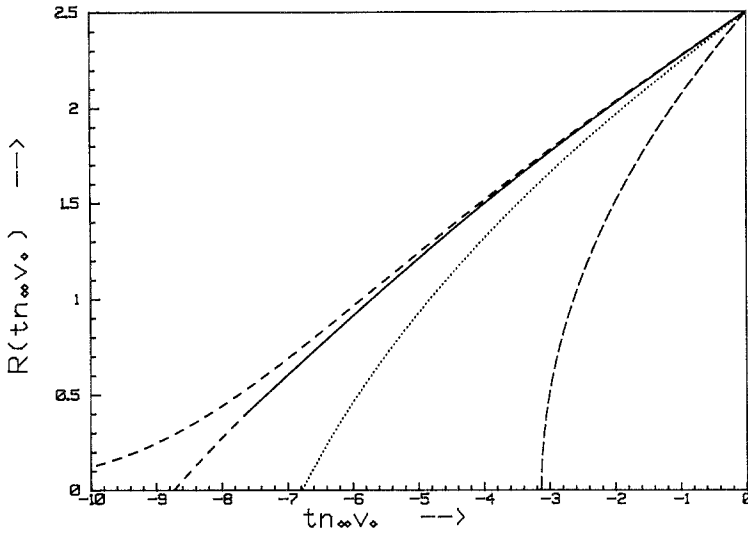


Fig. 3. Growth curves for the droplet radius, in velocity persistence lengths, as functions of $t n_\infty v_0$, with n_∞ the density of the vapor at $r = \infty$, v_0 the volume per particle in the liquid, and t measured in units of the velocity relaxation time, as calculated with our successive approximations to the reaction rate $k(R)$. The upper dashed, dotted, lower dashed, and solid curves are calculated using the corresponding approximations shown in Fig. 1. The dashed continuation of the solid curve was calculated using the tangent interpolation also shown there. For a finite saturation density n_s one can replace n_∞ by $n_\infty - n_s$.

low in any case), the requirement that the droplet can be in equilibrium with a vapor of the saturation density n_s leads to the boundary condition

$$P(u_r, u_t, R) = n_s \phi_0(u_r) \chi_0(u_t) \quad \text{for } u_r > 0 \tag{6.4}$$

instead of (4.16). This boundary condition is satisfied by the distribution

$$P_{n_s}(u_r, u_t, r) = P_M(u_r, u_t, r) + n_s \Psi_0(u_r, u_t, r) \tag{6.5}$$

Since only the component P_M carries a current, the resulting growth law simply becomes

$$\frac{dR}{dt} = \frac{Dv_0(n_\infty - n_s)}{R + \alpha_0^0 l + \alpha_1^0 R^{-1} l^2 + \alpha_2^0 R^{-2} l^3 + \dots} \tag{6.6}$$

i.e., only the excess of n_∞ over n_s contributes to the growth, as was to be expected. Equation (6.6) also describes the shrinking of droplets in under-saturated vapor. As a further step toward a more realistic description, one might include surface tension effects via an R dependence of n_s .⁽¹⁸⁾ Whether this makes sense depends on the magnitude of other neglected effects, some of which we shall list in the next and final section.

7. CONCLUDING REMARKS

The main advantage of our approach, as compared to earlier treatments, is its systematic nature. Our procedure itself determines which moments contribute in each order; in each order, the boundary condition is satisfied exactly, and the coefficients obtained are also exact, at least in principle.

Mathematically, the main open question is the convergence of the expansion in R^{-1} . The series (3.2) for the current solution is certainly divergent for some of its arguments, and similar divergences can be expected for the series (3.4a) for the boundary layer eigenfunctions. In our treatment the multiple summations (in particular those over n and i) are rearranged; this may improve the convergence, at least for certain moments of the distribution function. The first evidence contained in Figs. 1 and 2 is at least compatible with this kind of behavior; some additional evidence might be obtained by evaluating a few more terms in the series. If a finite radius of convergence is indicated, or if the series turns out to be asymptotic and of little use for small R , a complementary expansion for small R would have to be devised, and one may hope for an overlap of the convergence regions (or of the regions where the series provide accurate approximations). Such an approach may also become necessary when higher order terms in the series become unreliable due to accumulating numerical roundoff errors (convergence of the series for all R requires a rather rapid decrease of the absolute values of the α_i^{nL} with i).

Physically, our model involves a number of idealizations, only some of which are essential for its solvability. The condition that all particles hitting the surface are absorbed can be relaxed. A formalism for including the effect of partial absorption, and of temperature differences between droplet and gas, is described in I; its extension to the spherical case is straightforward. We note, however, that a sticking coefficient depending on u_r gives rise to an infinite set of coupled equations for the χ_i moments of the distribution function. Fortunately, experiments indicate (see, e.g., ref. 20) a sticking coefficient depending almost solely on u_r , at least for sticking to solid surfaces. A spectrum of reemitted particles deviating too strongly from a Maxwellian for high $|\mathbf{u}|$ might also give rise to convergence difficulties^(7,16) in the numerical treatment.

Especially for small droplets, effects of the heat of condensation may be important. They lead to an R -dependent temperature profile in the gas and to a temperature jump between the droplet and the surrounding gas mixture. Such effects also occur when one applies the model to particles that undergo chemical reactions at the surface (diffusion of oxidants to burning droplets). The effects of a temperature profile on the Klein-

Kramers equation were studied in a recent paper.⁽²¹⁾ They are readily incorporated into the present treatment, at least when the temperature profile is a simple function of r^{-1} , and the friction coefficient is a simple function of the temperature. In principle, the temperature jump at the surface will give rise to a kinetic boundary layer *in the medium*, in which the temperature profile is far from simple. This can be neglected, however, when the velocity persistence length of the Brownian particles is large compared to the mean free path for a particle of the background gas (which determines the size of the thermal kinetic boundary layer).

The most serious restriction on the applicability of our model is the assumption of free Brownian dynamics. This means that the mass ratio between the vapor molecules and those of the background gas must be large, and that the concentration of the vapor must be low. In addition, hydrodynamic backflow effects, which give rise to long-time tails in the velocity autocorrelation functions, are neglected; this means that the medium must have a specific weight low compared to that of the Brownian particles. This will be the case for not too dense gases, but not in general for fluids. When one or more of the above conditions are violated, one has to use a less simple kinetic equation, e.g., the (linearized) Boltzmann equation for a gas or a gas mixture. The construction of boundary layer solutions becomes much less simple, mainly because the collision operator (the analogue of our $\mathcal{C}_v + \mathcal{C}_r$) does not separate into operators acting on u_r and u_t only. Also, the number of variables in the hydrodynamic description (applicable far from the droplet) increases, and there are convective as well as diffusive contributions to heat and mass transport. In such cases one may still use moment methods like the ones used in ref. 9. A comparison between moment methods for the Brownian motion case and our more systematic treatment may be of some help in assessing the reliability of the former for more complicated kinetic equations.

ACKNOWLEDGMENT

This work was supported by the Fonds zur Förderung der wissenschaftlichen Forschung in Österreich.

REFERENCES

1. M. von Smoluchowski, *Phys. Z.* **17**:557, 585 (1916).
2. P. E. Wagner, in *Aerosol Microphysics II*, W. H. Marlow, ed. (Springer, Berlin, 1982), p. 129.
3. O. Klein, *Ark. Mat., Astron. Fys.* **16**(5):1 (1922); H. A. Kramers, *Physica* **7**:284 (1940).
4. C. Cercignani, *Theory and Application of the Boltzmann-Equation* (Scottish Academic Press, Edinburgh, 1975).

5. T. W. Marshall and E. J. Watson, *J. Phys. A* **18**:3531 (1985); **20**:1345 (1987).
6. P. S. Hagan, C. R. Doering, and C. D. Levermore, *SIAM J. Appl. Math.*, to be published.
7. M. E. Widder and U. M. Titulaer, *J. Stat. Phys.*, to be published.
8. K. Razi Naqvi, K. I. Mork, and S. Waldenstrøm, *Phys. Rev. Lett.* **49**:271 (1983).
9. V. Kumar and S. V. G. Menon, *J. Chem. Phys.* **82**:917 (1985).
10. D. C. Sahni, *J. Colloid Interface Sci.* **91**:418 (1983); **96**:560 (1983).
11. C. W. Misner, K. S. Thorne, and J. A. Wheeler, *Gravitation* (W. H. Freeman, San Francisco, 1970).
12. G. R. Kneller and U. M. Titulaer, *Physica* **129A**:81 (1984).
13. U. M. Titulaer, *Physica* **91A**:321 (1978).
14. C. D. Pagani, *Boll. Un. Mat. Ital.* **3**(4):961 (1970).
15. M. A. Burschka and U. M. Titulaer, *J. Stat. Phys.* **25**:569 (1981).
16. M. E. Widder, Diploma Thesis, Linz University (unpublished).
17. R. Beals and V. Protopopescu, *J. Stat. Phys.* **32**:565 (1983).
18. L. D. Landau and E. M. Lifshitz, *Statistical Physics, Part 1*, 3rd ed., E. M. Lifshitz and L. P. Pitaevskii, ed. (Pergamon, Oxford, 1980), §156.
19. S. Waldenstrøm and R. Razi Naqvi, *Ark. Fys. Sem. Trondheim*, No. 4, 1988.
20. K. D. Rendulic, G. Anger, and A. Winkler, *Surface Sci.* **208**:404 (1989).
21. M. E. Widder and U. M. Titulaer, *Physica A* **154**:452 (1989).